

PAPER • OPEN ACCESS

Applying a potential difference to minimise damage to carbon fibres during carbon nanotube grafting by chemical vapour deposition

To cite this article: David B Anthony *et al* 2017 *Nanotechnology* **28** 305602

View the [article online](#) for updates and enhancements.

Related content

- [Growth of long and aligned multi-walled carbon nanotubes on carbon and metal substrates](#)
M Delmas, M Pinault, S Patel et al.
- [Materials made of carbon nanotubes. The carbon nanotube forest](#)
Eduard G Rakov
- [Highly efficient growth of vertically aligned carbon nanotubes on Fe–Ni based metal alloy foils for supercapacitors](#)
Raja Noor Amalina Raja Seman, Mohd Asyadi Azam and Mohd Ambri Mohamed



Discover **Nanoparticle Solutions** for Exploratory Research
Find out more at **AVS International Symposium**
Florida, USA - booth 601

NanoGen
Nanocluster Sources

MANTIS
Partnered with SIGMA Surface Science

Applying a potential difference to minimise damage to carbon fibres during carbon nanotube grafting by chemical vapour deposition

David B Anthony^{1,2,3} , Hui Qian¹, Adam J Clancy¹ ,
Emile S Greenhalgh³ , Alexander Bismarck^{2,4}  and Milo S P Shaffer¹ 

¹Nanostructured Hierarchical Assemblies and Composites (NanoHAC) Group, Department of Chemistry, Imperial College London, London SW7 2AZ, United Kingdom

²Polymer and Composite Engineering (PaCE) Group, Department of Chemical Engineering, Imperial College London, London SW7 2AZ, United Kingdom

³The Composites Centre, Department of Aeronautics, Imperial College London, London SW7 2AZ, United Kingdom

⁴Polymer and Composites Engineering (PaCE) Group, Institute of Materials Chemistry, Faculty of Chemistry, Universität Wien, A-1090 Wien, Austria

E-mail: m.shaffer@imperial.ac.uk

Received 2 March 2017, revised 25 April 2017

Accepted for publication 8 June 2017

Published 7 July 2017



CrossMark

Abstract

The application of an *in situ* potential difference between carbon fibres and a graphite foil counter electrode (300 V, generating an electric field ca $0.3\text{--}0.7\text{ V }\mu\text{m}^{-1}$), during the chemical vapour deposition synthesis of carbon nanotube (CNT) grafted carbon fibres, significantly improves the uniformity of growth without reducing the tensile properties of the underlying carbon fibres. Grafted CNTs with diameters $55\text{ nm} \pm 36\text{ nm}$ and lengths around $10\text{ }\mu\text{m}$ were well attached to the carbon fibre surface, and were grown without the requirement for protective barrier coatings. The grafted CNTs increased the surface area to $185\text{ m}^2\text{ g}^{-1}$ compared to the as-received sized carbon fibre $0.24\text{ m}^2\text{ g}^{-1}$. The approach is not restricted to batch systems and has the potential to improve CNT grafted carbon fibre production for continuous processing.

Supplementary material for this article is available [online](#)

Keywords: carbon fibre, carbon nanotube, synthesis, chemical vapour deposition, potential difference enhanced

(Some figures may appear in colour only in the online journal)

1. Introduction

Carbon nanotubes (CNTs) have received significant attention due to their impressive intrinsic mechanical, thermal and electrical properties [1], leading to their incorporation into a wide

range of applications, including electrodes in fuel cells and batteries [2], sensors [3], catalyst supports [4], and microscopy probes [5]. One possibility is their use as primary reinforcements in a new generation of high performance structural materials [6, 7]; however, in the nearer term it may be more straightforward to use them to improve the response of the existing state-of-the-art carbon fibre-reinforced composites, by addressing matrix and interface dominated failures [8, 9].

There are two methods to incorporate CNTs into fibre reinforced matrices; one is to infiltrate CNT-loaded resins into



Original content from this work may be used under the terms of the [Creative Commons Attribution 3.0 licence](#). Any further distribution of this work must maintain attribution to the author(s) and the title of the work, journal citation and DOI.

conventional fibre preforms, the other alternative is to grow or coat CNTs onto the fibre surface before incorporation into a conventional resin matrix. The former method is usually limited to relatively low CNT loading fractions (approx. 2 wt%), due to the significant increase in matrix viscosity and filtration effects against the fibre preform above the rheological percolation threshold [10], despite recent progress [11]. For the latter method, CNTs can be attached to a fibre through various processes, including, chemical grafting [12–14], electrophoretic deposition [15, 16] and using a CNT-loaded fibre size [17]. However, these approaches are less desirable due to poor orientation and lack of strong attachment of the CNTs to the fibre surface. For use as a reinforcement in conventional matrices, direct synthesis of CNTs onto conventional structural fibres is preferred and provides specific reinforcement of the critical fibre–matrix interface. Carbon filament growth (analogous to carbon nanofibres) on single crystal graphite substrates was first reported by Baker *et al* [18] in the 1970s and later extended to carbon fibre supports by the same author [8]; interest has increased in recent years [19–29] with CNTs synthesised on silica or alumina fibres [22, 30–36] receiving greater attention due to greater stability of the catalyst on the surface. Once embedded in resin, CNT-grafted fibres (also referred to as fuzzy fibres [37–39] or hairy fibres [7]) have been shown to increase interfacial shear strengths. Although values vary widely, the largest improvements reported for single fibre pull-out (carbon fibre) and single fibre fragmentation (silica fibre) tests are 94% [40] and 156% [32] over as-received unsized and as-received sized baselines, respectively. When applied to woven fabric preforms (in this instance, pyrocarbon coated carbon fibres), the presence of CNTs in the interfacial region have been reported to increase the interlaminar shear strengths by up to 209% [41].

Carbon fibres out-perform silica and alumina fibres in terms of stiffness and specific properties; however, when carbon fibres are used as substrate for chemical vapour deposition (CVD) CNT growth, they are readily damaged, reducing strength in particular. A number of possible degradation mechanisms may occur; fundamentally, the carbon needed for CNT growth may be partly derived from the parent carbon fibre substrate itself (instead of the intended hydrocarbon), leading to substrate carbon dissolution into catalyst particles or the pitting of the fibre surface, historically referred to as ‘channelling’ in gasification experiments [42]. If residual water/oxygen is present, or if hydrogen is used as a catalyst reducing agent, then hydrolysis [43] or hydrogenation/gasification [44] of the carbon substrate may occur during high temperature CVD, particularly in the presence of a catalyst. Controlling the CNT-synthesis on carbon fibre through optimised gas stoichiometry [45] with reduced temperature (ca 500 °C) [21, 46], reduces fibre damage due to the less harsh synthesis conditions, however, the quality of the resulting CNTs tends to be lower. One alternative strategy to limit damage relies on the use of catalysts which do not readily dissociate carbon, for example ZrOCl [47] or Cu [48],

although these systems are likely to grow herringbone or platelets carbon nanofibres rather than multiwalled nanotubes. Other routes include prolonged exposure to CVD conditions to allow sustained damage to the graphitic lattice to be repaired [20], or conversely through short CNT growth duration, ca 15–20 min, to minimise damage sustained during synthesis [49–51]. Some researchers have suggested that maintaining the carbon fibres under tension during CNT synthesis reduces thermally-activated mechanochemical changes in the fibre microstructure [19]. Perhaps the most widely used strategy to circumvent damage to the carbon involves the application of barrier coatings, often pyrolytic carbon [52, 53], alumina [54, 55] or silicon/silica based [56–63], which limit/prevent undesired dissociation of catalyst and/or improve catalyst loadings. However, this approach is likely to create a new weak interface, limiting the mechanical benefits in use. The nature of the underlying surface can also influence the quality of the CNTs grown, for example, a graphitic carbon substrate is reported to produce more graphitic CNTs [64, 65].

Controlled CNT alignment is especially relevant for their application in composites [7], and can be introduced during synthesis, for example via gas flow [66], lattice-/step-orientated growth effects [67, 68], steric interactions during dense forest growth [69], or electric fields generated either intrinsically during plasma-enhanced CVD (PE-CVD) [70–73] or independently [66, 74–79]. Gas flow and lattice-orientated growths can only be applied to relatively low concentrations of CNTs, and tend to generate alignment parallel to the substrate. Independent field generation during thermal CVD has an advantage over PE-CVD approaches which can etch both carbon fibres and CNTs [80]. Simple electric fields generated by applying a potential difference to relevant electrodes can also be applied to systems without the stringent low-pressure conditions required for stable plasma generation. The application of a static field is usually applied in a parallel plate capacitive configuration without significant current flow; an alternating field embodiment is also reported [81].

Resistive or ohmic heating, has been previously shown to synthesise CNTs on carbon paper [82] and pitch based carbon fibres [83], as a variation of cold-walled CNT CVD synthesis. In an ohmically heated configuration, electrical current flows through a resistive substrate generating the temperatures required for CNT CVD growth. However, this approach is not designed to generate a significant electric field around the fibres, and no alignment is expected or reported.

A desirable carbon nanotube-grafted-carbon fibre (CNT-g-CF) product for structural composites has aligned, dense grafted CNTs, approximately normal to the carbon fibre substrate in a radial configuration, and a relatively short length consistent with maintaining a high primary fibre volume fraction in the final material. The process should avoid damaging the carbon fibres and be in principle scalable to continuous production. The aim of this study was to apply a potential difference between the carbon fibre substrate and a cylindrical counter electrode, to generate a static electric field

during atmospheric pressure hot-walled CVD. In particular, the CNT-g-CF approach may provide a practical route to achieve the desired growth of aligned CNTs normal to the fibre axis. In this embodiment, there is no intention to generate plasma, only to charge the substrate, to spread the carbon fibre tow and to encourage aligned CNTs growth from the carbon fibre surfaces.

2. Experimental

2.1. Materials

Sized polyacrylonitrile (PAN)-based carbon fibres, AS4C-GP-12K-8, HS-CP-4000 grade, continuous 12k fibre tow were used. The carbon fibres have a circular section fibre diameter of $6.9 \mu\text{m}$ ⁵. They were kindly supplied by Hexcel, UK. A mixture of iron(III) nitrate nonahydrate ($\geq 98\%$ ACS reagent, Sigma-Aldrich, UK) and nickel(II) acetylacetonate ($\geq 98\%$, VWR, UK) in ethanol (EtOH, $>99.7\%$ BDH Pro-labo, VWR, UK) was used to prepare the bi-catalyst precursor solution. A mixture of Ni-Fe catalyst has been shown to have increased activity (channelling rate) in gasification experiments in the presence of hydrogen [42]. Argon gas (99.998 vol% minimum, zero grade), premixed hydrogen in argon (Ar $90 \pm 0.5 \text{ vol}\%$ and H_2 $10 \pm 0.5 \text{ vol}\%$) and acetylene (C_2H_2 , 98.5 vol% minimum) were used in CVD CNT synthesis, all at a pressure of 2 bar. All gases were purchased from BOC Gases, UK. Graphite foil (99.8%, C1179, Advent Research Materials Ltd, UK) of approximate dimensions $100 \text{ mm} \times 180 \text{ mm} \times 0.2 \text{ mm}$ was used as a counter electrode. High-performance liquid chromatography (HPLC) EtOH (95%–97% HiPerSolv CHROMANORM, VWR, UK) was used for the ultra-sonication experiment. All chemicals and the carbon fibres were used as-received.

2.2. Catalyst precursor deposition on carbon fibres

Carbon fibre tows were impregnated with catalyst precursor by submerging them for 2 min into a bi-catalyst precursor solution comprising of 2 wt% iron(III) nitrate nonahydrate and 2 wt% nickel(II) acetylacetonate in ethanol to give a molar ratio of Fe:Ni/1:1.6. The fibres were then dip washed in deionised water (18 M Ω) for 1 min, then dried at standard ambient atmospheric temperature and pressure.

2.3. Synthesis of CNT-grafted-carbon fibres

Thermal CVD was performed on 10 cm lengths of carbon fibre tow (each tow was split into sections each containing approximately 4000 fibres), which had been coated with bi-catalyst precursor, in a hot-walled CVD set-up using a 2' quartz tubular furnace (PTF 15//610, Lenton, UK), joined using quick connect tube adaptors (LewVac LLP, UK). Custom made quartz frames (Robson Scientific, UK) were used to hold the fibres in position in the furnace tube thus

maintaining accessibility to the gas flow. The frames were held in place by gravity. The fibre regions that had been occluded by the frames were not characterised. The chamber was purged with argon for at least 40 min (500 sccm for 20 min, then 1000 sccm for 20 min) prior to heating to $770 \text{ }^\circ\text{C}$ at $10 \text{ }^\circ\text{C min}^{-1}$ under argon flow (500 sccm). The synthesis temperature was chosen to be above the bulk phase eutectoid point of Fe-C, $723 \text{ }^\circ\text{C}$ at 0.83 wt% C [84]. The temperature of the eutectoid point of Ni-Fe is $347 \text{ }^\circ\text{C}$ at 49 at% Ni in Fe [85] and was exceeded during the reaction, but the temperature of the eutectoid point for Ni-C (at 3 at% C, $1326 \text{ }^\circ\text{C}$) was not attained [86]. The gas was then replaced with premixed hydrogen in argon (2000 sccm, for catalyst reduction) for 10 min prior to the addition of acetylene (10 sccm, carbon feedstock for CNT-growth) for 60 min. Once the reaction had been completed, the acetylene source was closed and the system was cooled in flowing premixed hydrogen in argon gas (2000 sccm) to $500 \text{ }^\circ\text{C}$, which was then replaced by argon (500 sccm) while cooling to $100 \text{ }^\circ\text{C}$. Samples were then left to cool overnight before removal from the furnace at room temperature. A schematic of the CVD batch set-up and mass flow controller details are shown in the supplementary information (S.1, figures SI 1(a), (b) and S.2 available online at stacks.iop.org/NANO/28/305602/mmedia).

To apply a potential difference *in situ* during the synthesis of CNT-g-CF, the arrangement was modified to establish an electrical connection to the carbon fibre and to a counter electrode introduced via an electrical-feed through (LewVac LLP, UK, figures 1(a) and (b)). Graphite foil was chosen as the counter electrode in the circuit as it is a conductive and flexible material, which does not catalyse the growth of CNTs and is thermally and chemically stable under reaction conditions. A sheet of compacted graphite foil was rolled into a cylinder and inserted into the 2" quartz tube where it was allowed to unroll to create a 2" inner diameter tubular counter electrode. Electrical connection to the counter electrode was made by piercing the graphite foil with a stainless steel wire (figure 1(c)). The electrical connection to the carbon fibre was made by wrapping a piece of graphite foil to the quartz frame then sandwiching the carbon fibres with cleaned stainless steel wire binding, which was then used as the connection wire (supplementary information S.1, figures SI 1(e) and S.3). The connecting wires were covered with ceramic beads (fish spine beads, RS Components Ltd, UK) to reduce the likelihood of shorting and an insulating piece of quartz ($36 \text{ mm} \pm 0.5 \text{ mm}$, wall thickness $1.5 \text{ mm} \pm 0.2 \text{ mm}$, Robson Scientific, UK) placed between the counter electrode and fibres to stop stray fibres from discharging the circuit (figures 1(a) and (b)). The potential difference was measured using a high voltage probe (TT-HVP 40, 1000:1 divider, division ratio accuracy 1%, Testec, Germany) connected to a voltmeter (IDM67, $\pm 0.7\%$ voltage, IEC 1010-1, ISO-Tech, UK). A 1:250 voltage amplifier (MM3P1.5/12, 1.5 W, 12 V input, linear high voltage output 3 kV max and 0.5 mA max, efficiency 55%–70%, Spellman High Voltage Electronics, UK) was used to increase the voltage output in conjunction with a variable current and voltage power supply source (Mastech HY3003D, variable DC supply, 30 V max and 3 A

⁵ Hexcel Composites, HexTow™ AS4C carbon fibre, Data Sheet (2009) 1–2.

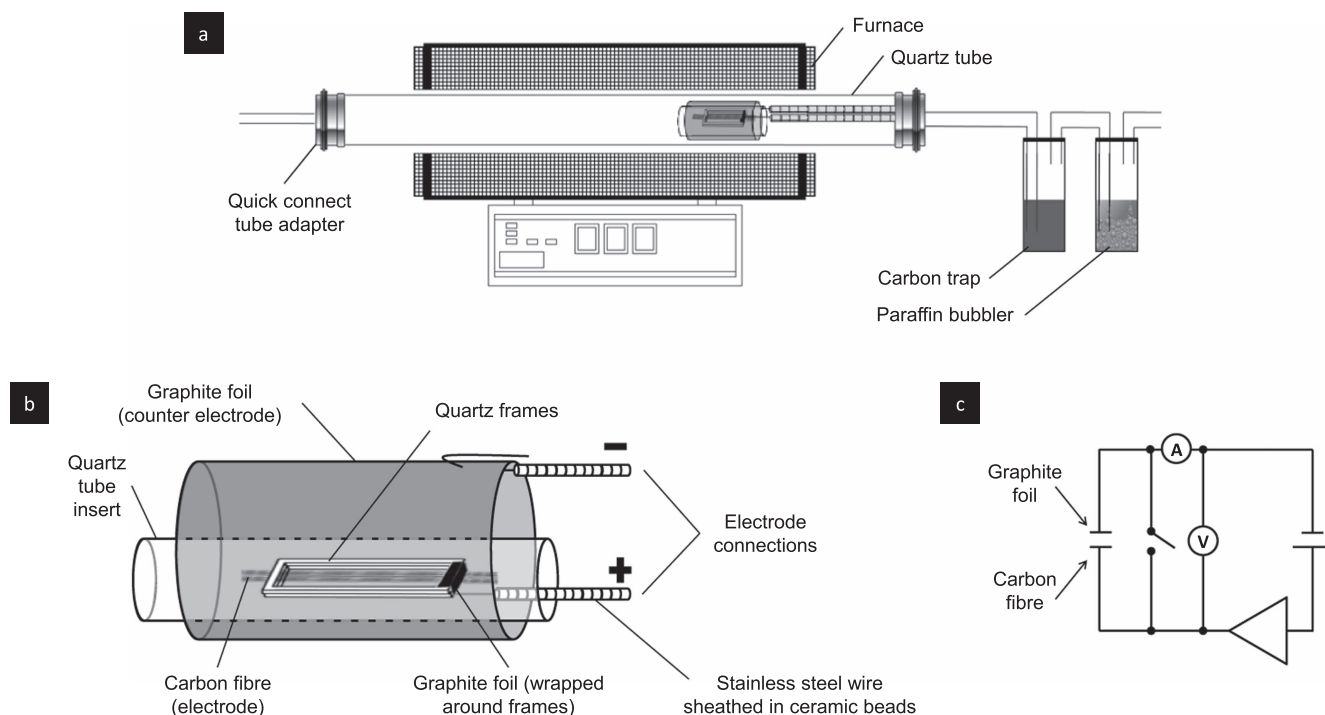


Figure 1. (a) Schematic illustration of the batch CVD set-up, with fibres held in quartz frames and electrical connections to the carbon fibre and graphite foil electrodes shown, (b) an enlarged sample region, (c) circuit diagram of the capacitor arrangement of the carbon fibre and graphite foil electrodes including a switch to aid discharge.

max output, Digimess Instruments Ltd, UK). The CNT-growth reaction conditions were identical to the precursor-loaded carbon fibres previously described (gas concentration/flow/temperature etc), except for the application of a potential difference. The potential difference was applied/discharged only under inert gas conditions to minimise any risk associated with accidental discharge. The potential difference applied to the carbon fibre substrate was +300 V with respect to the counter electrode (graphite foil, earthed) with the electric-field estimated to be of the order of $0.3\text{--}0.7\text{ V }\mu\text{m}^{-1}$, with further details contained in the supplementary information S.4.

2.4. Fibre morphology characterisation

As-received sized fibres, bi-catalyst coated fibres, and CNT-g-CF were examined with a high resolution field emission gun scanning electron microscope (SEM) (5 kV, Leo Gemini 1525 using SmartSEM software interface V05.05.03.00, Carl Zeiss NTS Ltd, UK). The SEM samples were prepared on Al stubs adhered with silver DAG, with all SEM preparation products sourced from Agar Scientific Ltd, UK. Transmission electron microscopy (TEM, JEOL-2010F Electron Microscope, JEOL Ltd, UK) was performed at 200 kV (Digital Micrograph V1.81.78 for GMS 1.8.0, 1996, Gatan Inc., USA software), on cut fibre specimens prepared in a folding TEM grid (butterfly, copper mesh, Agar Scientific Ltd, UK), folded and fixed into position using the provided latch. Post processing of the microscopy images to determine the feature dimensions was carried out using open-

source Java software ImageJ (V. 1.45s, US National Institutes of Health, USA [87]).

2.5. Characterisation of fibre tensile properties and CNT adhesion

Characterisation of the CNT-g-CF was carried out via single fibre tensile tests, using a TST350 Tensile Stress Tester and computer interface (Linksys32, V1.9.1, Linkam Scientific Instruments Ltd, UK) following the British standard BS EN ISO 11566, 1996 [88] Method B, compliance value (K) 16.6 mm N^{-1} , using $6.9\text{ }\mu\text{m}$ diameter for all samples (see footnote 5) (N.B. orthogonal CNT forests do not carry any appreciable tensile load in this test, so all force applied during single fibre tensile loading are assumed to be solely attributable to the carbon fibre's properties. No significant alteration to the core fibre diameters during processing was observed figure 3(b)), $15\text{ }\mu\text{m s}^{-1}$ crosshead speed, in standard ambient atmospheric temperature and pressure using a 20 N load cell, as described elsewhere [25]. Fibres were glued to card holders using epoxy adhesive (Araldite Rapid Adhesive, Huntsman Advanced Materials GmbH, CH) and tested at gauge lengths of 15, 25 and 35 mm. Gauge-length independent mean fibre strength fits are included in results (Weibull shape, OriginPro 8.6.0 programme, Score method Blom, OriginLab Corp., USA, 2012) [89]. Single fibre tensile tests were carried out to determine the effect of CNT-grafting on the fibre properties. To investigate the adhesion between the grafted CNTs and carbon fibres, qualitatively, CNT-g-CF were bath sonicated in EtOH [27, 90, 91]. A 4 cm section was cut from the CNT-g-CF tow,

left to soak in HPLC EtOH (5 ml) for 1 h then bath sonicated (USC 300 T, 45 kHz, VWR UK) in a small vial for 1 h at a temperature of 30 °C.

2.6. Surface area characterisation

The specific surface areas of as-received sized, bi-catalyst coated fibres, and CNT-g-CF were determined using Brunauer, Emmett and Teller (BET) theory following the ISO 9277 standard [92] using Micromeritics TriStar Surface Area and Porosity Analyser and TriStar3000 V6.07 software (Micromeritics UK Ltd, UK) with oxygen-free nitrogen (99.998 vol%, BOC, UK). CNT-g-CF (0 V, without a potential difference applied during the synthesis) were assessed using krypton (99.999 vol%, BOC, UK) due to the low surface area and mass. Prior to a measurement, the samples were degassed in nitrogen for at least 4 h at 80 °C, BET isotherms can be found in the supplementary information, S.5

2.7. Raman spectroscopy characterisation

Raman analysis provides a powerful non-destructive method to assess the sample structure and imperfections (defects), particularly of graphitic materials [93]. The intensity ratio of the G mode (1582 cm^{-1}) to the D mode (1350 cm^{-1}) (I_G to I_D) ratio is often used to characterise the level of disorder in a sp^2 (graphene) framework. Raman spectroscopy was carried out on a LabRAM Infinity with 532 nm [2.33 eV] Nd-YAG green laser (LabSpec V4.18-06, 2005 software interface, Horiba Jobin Yvon Ltd, UK) in a backscattered geometry. Measured Raman spectra were background subtracted, with five spectra taken at different fibre locations, normalised to the G mode and averaged.

2.8. Thermal gravimetric analysis (TGA)

TGA was performed to evaluate the weight of synthesised CNTs; thermogram fittings and details can be found in the supplementary information S.6. TGA was carried out on a Mettler Toledo TGA/DSC 1 with a GC200 flow controller, using STARe software v12.00 C. Under nitrogen (60 sccm) samples were heated from 30 °C–100 °C at 35 °C min^{-1} , and then held isothermally at 100 °C for 30 min to dry, then the gas was changed to compressed air (60 sccm) and the temperature was then increased to 850 °C at 10 °C min^{-1} .

3. Results

3.1. Microscopy and morphology

The attempted synthesis of CNT-g-CF with no applied potential difference (0 V) figures 2(a)–(d), produced only sporadic CNT-growth and caused severe pitting on the carbon fibre surface (see figure 2(a)) associated with a slight reduction in carbon fibre diameter (measured by SEM, table 1). When carbon fibres were subjected to a 300 V potential difference during CNT synthesis, figures 2(e)–(h), a significant

increase in the number of CNTs grown on the carbon fibres surface was observed, with the CNT-g-CFs exhibiting a dense forest-like morphology. In areas where the CNTs had been pulled away from the fibre surface during SEM preparation of CNT-g-CF (300 V) no observable damage associated with the growth of CNTs was identified (figure 3). TEM images (figure 2(h)) of CNTs synthesised on the surface of the carbon fibres, with an applied potential, showed that the nanotubes had grown in a random orientation, were multi-walled, and had a relatively disordered internal structure akin to full core multi-walled CNT [94] (measured via TEM, table 1). Catalyst was observed both at the tips and the bases of the CNTs, so the dominant growth direction was unclear. The average external diameter of isolated CNT-g-CF (300 V) increased significantly to $26\text{ }\mu\text{m} \pm 7.8\text{ }\mu\text{m}$ (measured via SEM, table 1), indicating a (minimum) radially resolved CNT-growth length of approximately $10\text{ }\mu\text{m}$. There was no discernible difference between CNT coverage/morphology on carbon fibres from the centre of the tow to that on the tow edge. In the core of the tow, neighbouring carbon fibres were on occasion completely enveloped by the growth of CNTs (supplementary information S.7, figure SI 6). SEM images of as-received sized and bi-catalyst precursor coated carbon fibres can be found in the supplementary information (S.8, figure SI 7). The reverse electrode configuration i.e. carbon fibre substrate earthed and graphite foil +300 V produced an identical CNT morphology (supplementary information S.9, figure SI 8).

3.2. Fibre tensile properties

Mechanical testing of CNT-g-CF (0 V) showed that the carbon fibres had significantly reduced tensile properties (figure 4, supplementary information, S.10, table SI 3) associated with damage caused by pitting of the catalyst particles into the carbon fibre surface. CNT-g-CF (300 V) had markedly superior tensile properties when compared to those of CNT-g-CF (0 V) and were similar to the as-received sized and bi-catalyst precursor deposited carbon fibre controls. The variability in the fibre strengths can be characterised by the Weibull shape parameter (Weibull modulus). All samples, with each sample set tested at three different gauge lengths, have a similar Weibull distribution with Weibull moduli of between 3.4–5.8. A Weibull modulus of around 5 is typical for carbon fibres [95]. It appears that the applied potential difference minimised the damage to the carbon fibres, possibly by isolating the catalyst particles on the surface. However, it is also important to note that the CNTs were well attached to the carbon fibres. The strength of the attachment was demonstrated, qualitatively, by ultrasonically CNT-g-CF (300 V) in ethanol; although the CNTs collapsed and were densified (figure 5) by the capillary forces during drying [96], they remained fully and uniformly attached, consistent with a direct bond with the carbon fibres.

CNT-g-CF without an applied p.d. (0 V)

CNT-g-CF with an applied p.d. (300 V)

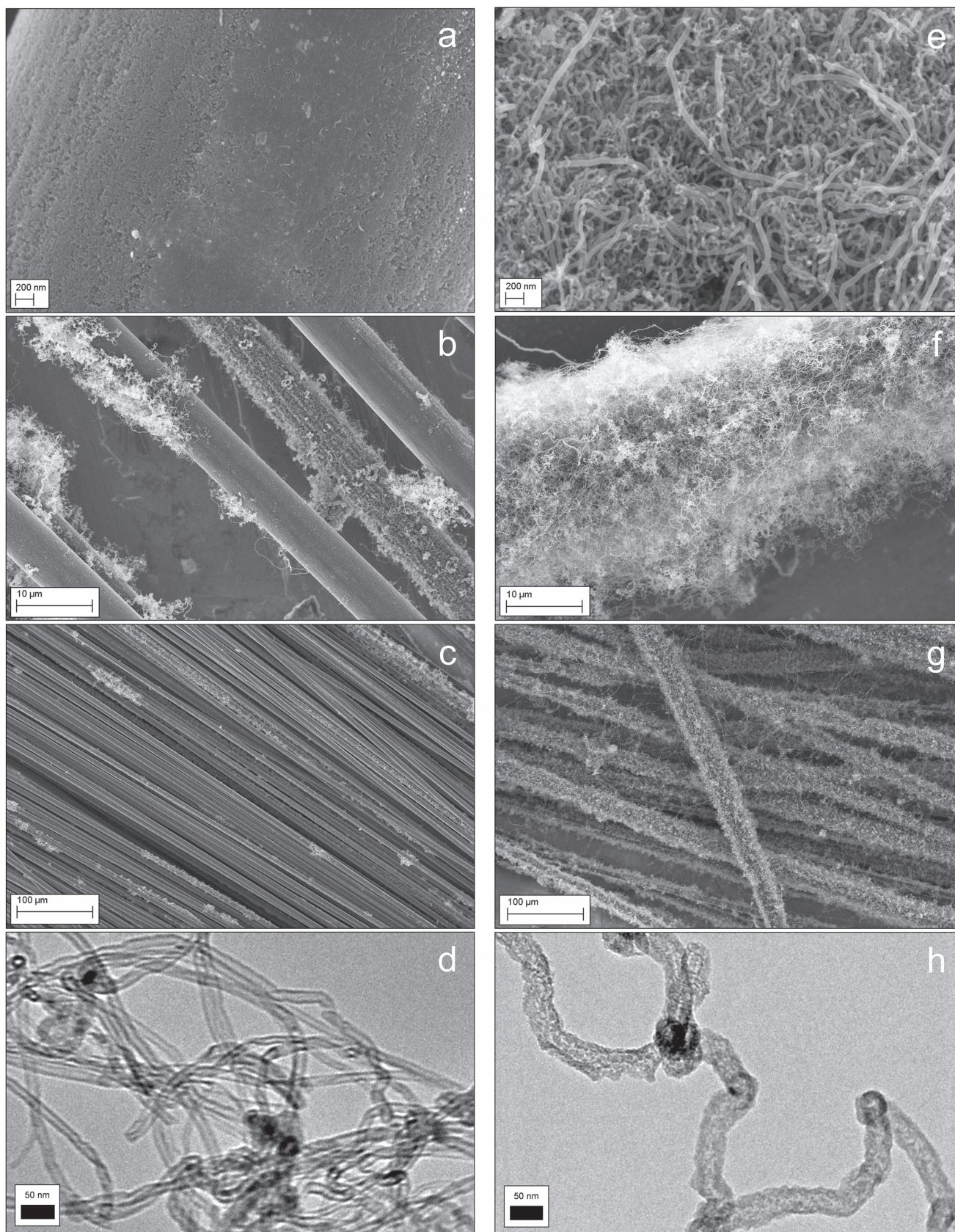


Figure 2. SEM images (a)–(d) TEM image of CNT-g-CF (0 V) synthesised without the application of a potential difference (p.d.). SEM images (e)–(h) TEM image of CNT-g-CF synthesised under an applied potential difference of 300 V. For electron micrographs of as-received sized carbon fibre and bi-catalyst coated carbon fibre refer to supplementary information S.8, figure SI 7.

Table 1. Carbon fibre and carbon nanotube dimensions/content deduced from microscopy, TGA and BET analysis.

Sample	Fibre diameter [†] (μm)	CNT perp. thickness to fibre [†] (μm)	CNT diameter [◇] (nm)	Specific surface area ($\text{m}^2 \text{g}^{-1}$)	CNT weight percentage [‡] (wt%)
As-received sized carbon fibre	6.9 ± 0.2	N/A	N/A	0.24 ± 0.005	N/A
Bi-catalyst precursor deposited carbon fibre	6.9 ± 0.2	N/A	N/A	0.31 ± 0.005	N/A
CNT-g-CF (0 V) without potential difference	6.5 ± 0.3	N/A	16 ± 6.4	0.47 ± 0.005	N/A
CNT-g-CF (300 V) with potential difference	26 ± 7.8	~ 10	56 ± 36	185 ± 0.6	< 37

Values with a [†], [◇] and [‡] refer to measurements made on the SEM, TEM and TGA (upper bound presented) respectively.

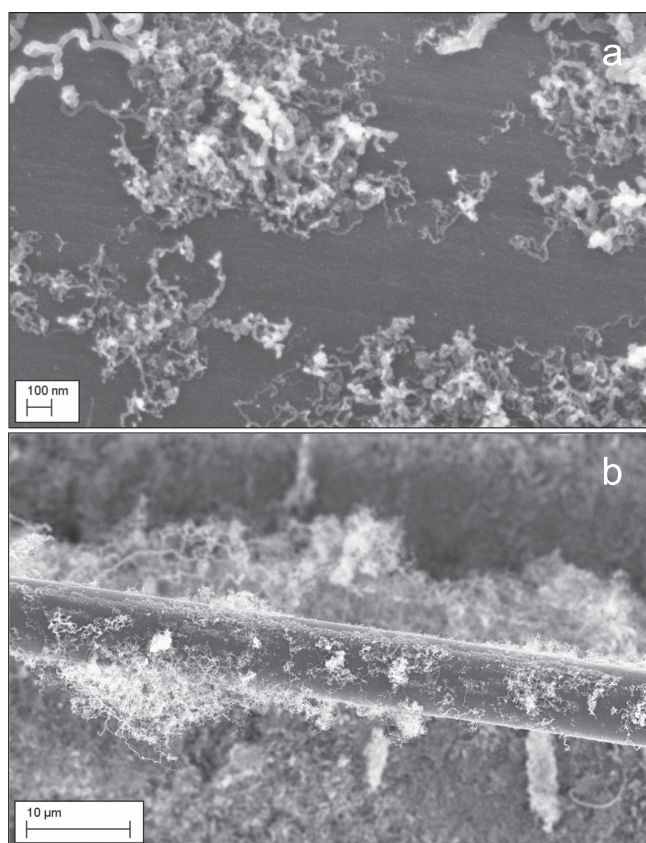


Figure 3. SEM images (a) and (b) of CNT-g-CF synthesised under an applied potential difference of 300 V, a carbon fibre has been pulled away from the tow after CNT synthesis with an exfoliated section, showing an apparently undamaged carbon fibre surface.

3.3. Surface area and TGA

The specific surface area (table 1) of the pristine carbon fibres was low ($0.24 \text{ m}^2 \text{g}^{-1}$) as was expected, and was not significantly increased by the deposition of the bi-catalyst precursor, nor by CVD in the absence of an applied potential difference. The surface area of CNT-g-CF (0 V) remained below $1 \text{ m}^2 \text{g}^{-1}$, consistent with the low yield of CNTs as seen under the SEM (figures 2(a)–(c)). In contrast, for the CNT-g-CF (300 V), the dense layer of grafted CNTs increased the surface area substantially ($185 \text{ m}^2 \text{g}^{-1}$). This value is greater than many literature values which are in the

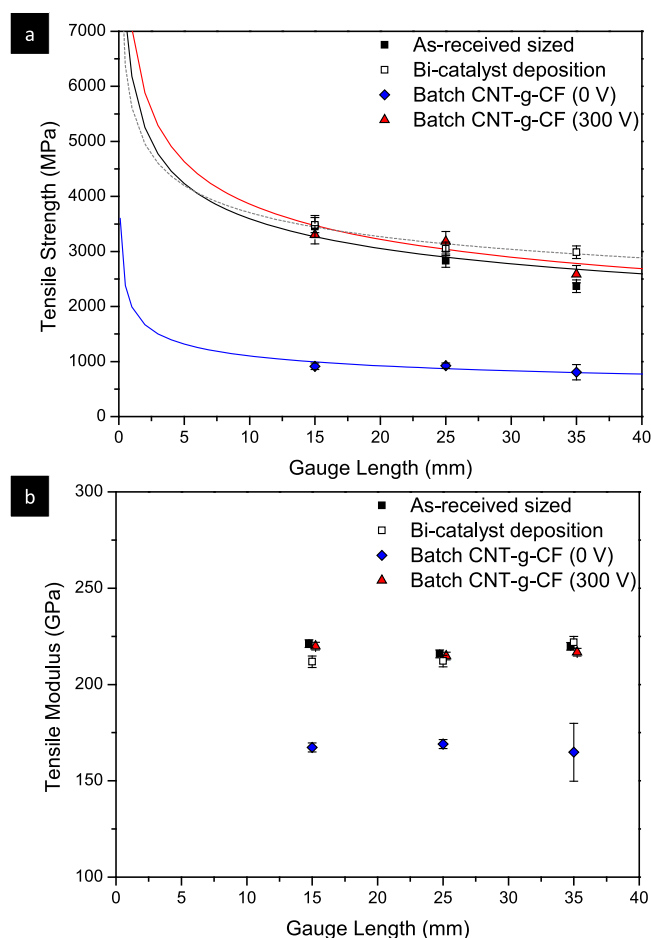


Figure 4. (a) Average tensile strengths (with gauge dependence fitted using the Weibull shape and scalar parameters) and (b) average tensile modulus of elasticity (tensile modulus, slightly offset on the abscissa for clarity), for CNTs grafted onto the fibre surface with (CNT-g-CF (300 V)) and without (CNT-g-CF (0 V)) the application of a potential difference. Tabulated data can be found in the supplementary information S.10 (a colour version of this figure can be viewed online).

region of $60\text{--}90 \text{ m}^2 \text{g}^{-1}$ for CNT-g-CF cloth [97, 98], indicative of a high degree of grafting throughout the tow. The surface area was naturally lower than typical commercially bought multi-walled CNTs (MWCNTs, $250 \text{ m}^2 \text{g}^{-1}$ [99]), due to the contributing mass of the carbon fibres. As-received sized carbon fibres, bi-catalyst deposited carbon fibres and CNT-g-CF (0 V) showed Type II adsorption isotherms related

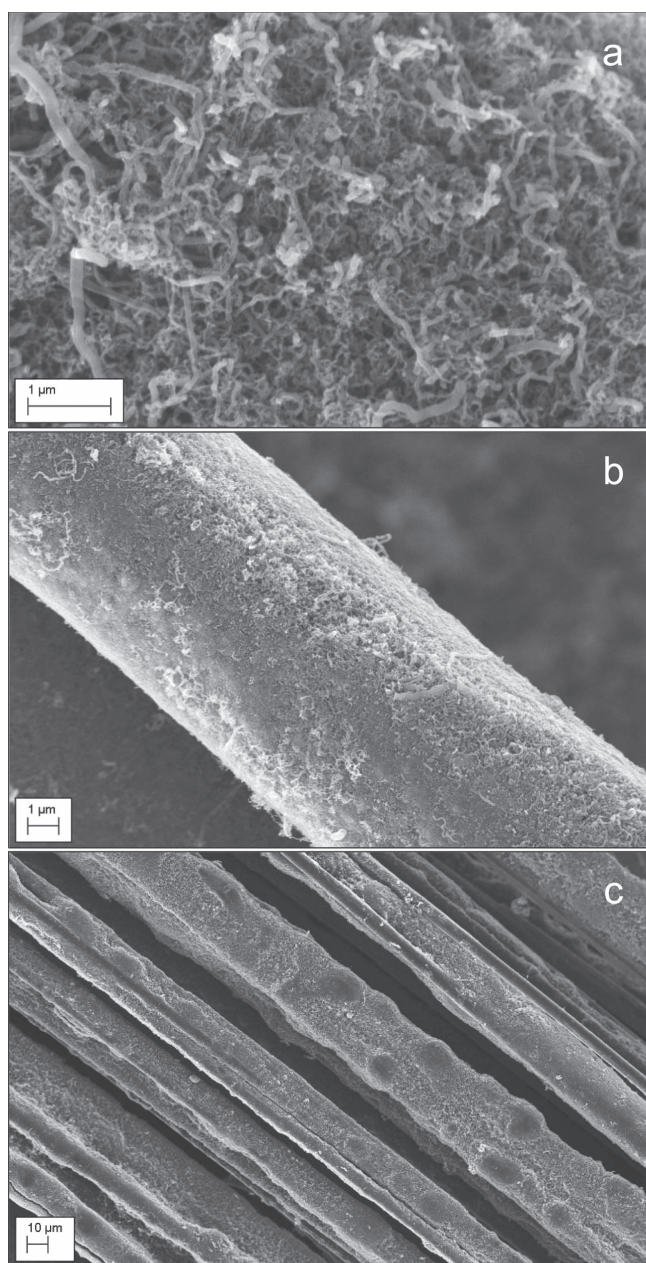


Figure 5. (a)–(c) SEM images of CNT-g-CF synthesised under an applied potential difference of 300 V after bath sonication for 1 h in EtOH, and then dried at room conditions, showing the compacted CNT forest still bound to the carbon fibre surfaces.

to a non-porous structure, with CNT-g-CF (300 V) showing a Type IV adsorption isotherm indicating that mesoporosity has been introduced through the grafted CNTs, in accordance with the IUPAC classification [100], BET isotherms contained in the supplementary information, S.5. TGA was used to estimate the weight percentage of CNTs in CNT-g-CF (300 V) sample through the de-convolution of the CNTs and carbon fibres decomposition features, indicating an upper bound of 37 wt%. No separate feature attributable to CNTs was observed for the CNT-g-CF (0 V) sample, although a lower decomposition temperature for the primary fibre due to damage may obscure a minor contribution. A full discussion

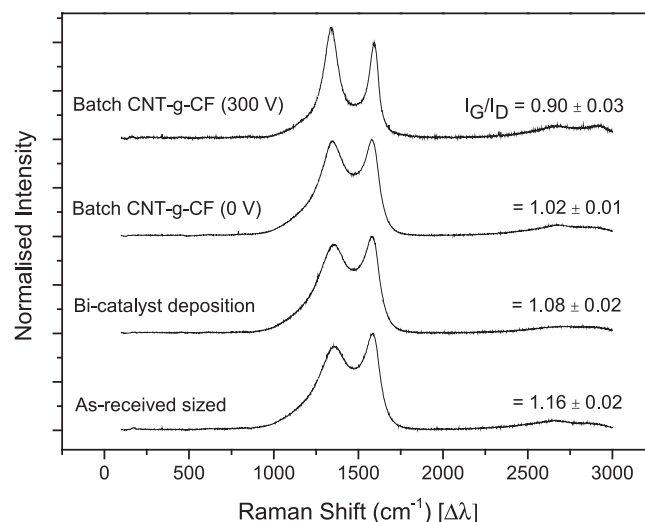


Figure 6. Raman spectra of as-received sized carbon fibres, bi-catalyst deposition on carbon fibres, and CNT-g-CF synthesised without (0 V) and with (300 V) a potential difference applied with corresponding I_G to I_D ratios shown.

of TGA analysis can be found in the supplementary information, S.6.

3.4. Raman spectroscopy analysis

As-received sized and bi-catalyst precursor coated carbon fibres showed characteristic PAN carbon fibre Raman spectra with D and G modes (figure 6). Distinct D, and G mode sharpening was observed for CNT-g-CF (300 V) synthesised with a potential difference, which was attributed to abundant CNT-growth on the surface (figures 6 and 2(e)–(h)) [101]. Nevertheless, the CNTs had relatively low crystallinity (low I_G/I_D ratio) which was expected from the disordered CNT structure observed in the TEM (figure 2(h)). The Raman spectrum for CNT-g-CF (0 V) did not display mode sharpening and was indistinguishable from controls, indicating an insignificant CNT contribution.

4. Discussion

The application of a potential difference altered and encouraged CNT-growth allowing high density coverage of CNTs uniformly across the entire fibre length. Importantly, there was no pitting or damage of the carbon fibre, as evidenced by the retention of thermal stability, and the mechanical properties in contrast to many previous CNT-g-CF production routes. Conversely, when no potential difference was applied during CVD, poor CNT synthesis and damage to the underlying carbon fibre structure was observed. The exact mechanism underlying the increased CNT-growth on a charged carbon substrate is not well established but is likely to include either altering the catalyst dissolution characteristics, Coulombic effects altering the catalytic activity/particle size, altering the catalyst wetting/mobility, improved gas flow through the fibre bundle, or a combination thereof. The

polarity of the potential difference applied to the system (carbon fibre as positive electrode or earth) did not influence the magnitude of CNT growth (nor the hierarchical structure of the forests) indicating that growth is a function of the absolute potential difference, rather than electric field. Non-Faradaic electrochemical modification of catalytic activity, can therefore be excluded [102], but electrowetting effects may influence the formation of uniform catalyst particles upon reduction of catalyst precursor under an applied potential [103–105].

There was no indication that improved CNT growth was due to plasma-enhancement; the voltage and current were relatively low (300 V and <0.01 A, respectively) and CVD was carried out at or slightly above atmospheric pressure, at conditions typically incompatible with generating or sustaining a plasma [106–108] (further discussion included in supplementary, S.11). During the process, the electrodes maintained a fixed potential difference, no characteristic plasma glow was observed and CNT-growth times were sufficiently long (60 min) that if a plasma were present, etching would be visible on both the carbon fibres and CNTs [80].

In all instances, CNT growth was disordered in spite of the presence of a high electric field, well known to induce orientation during typical CNT growth. The minimum estimated field strength of $0.27 \text{ V } \mu\text{m}^{-1}$ in this experiment is higher than that reported as a threshold ($0.1 \text{ V } \mu\text{m}^{-1}$) for CNT alignment [109, 110]. It is thought that the complex electric fields produced between the carbon fibres within the ca 4000 fibre bundle alter the local conditions. Growth on isolated and individualised fibres might allow for symmetric fields and have idealised radial growth; however, this approach would lack scalability for composite applications.





5. Conclusion

In conclusion, the application of a potential difference has been shown to enhance the uniformity of CNTs grown directly on carbon fibres. Crucially, in addition, the modified procedure limits any damage to the carbon fibre substrate that degrades the intrinsic mechanical properties observed in most CVD grafting experiments. The use of CNT-grafted-carbon fibres as hierarchical reinforcements in composites is expected to improve transverse mechanical properties, as well as multifunctional properties including electrical/thermal conductivities. In this context, establishing a growth process which avoids degrading the primary fibre properties is vital. In contrast to previous routes which either heavily damage the carbon fibre surface or require a coating/protective barriers (which both dramatically hinder final composite performance), here the intrinsic fibre properties are maintained. Furthermore, the application of a potential difference to the carbon fibre substrate is a viable option to effectively improve CNT-growth which might be applied to other chargeable substrates (carbonaceous or otherwise).

Acknowledgments

The authors would like to thank the UK Engineering and Physical Sciences Research Council (EPSRC) (EP/P502500/1) and to EPSRC Impact Acceleration: Pathways to Impact Award (EP/K503733/1) for the financial support of this work and Hexcel for supplying the AS4 carbon fibres. Dr Stephen A Hodge, Dr Robert Menzel and Dr Jodie Melbourne (NanoHAC Group, Imperial College London) are acknowledged for their help with TEM, and Dr Matthew E P Markiewicz for assistance with BET (Kucernak Research Group, Imperial College London). All underlying data to support the conclusions are provided within the manuscript or electronic supplementary information.

ORCID

David B Anthony  <https://orcid.org/0000-0002-4032-008X>
 Adam J Clancy  <https://orcid.org/0000-0002-1791-8999>
 Emile S Greenhalgh  <https://orcid.org/0000-0002-3923-2883>
 Alexander Bismarck  <https://orcid.org/0000-0002-7458-1587>
 Milo S P Shaffer  <https://orcid.org/0000-0001-9384-9043>

References

- [1] Dresselhaus M S, Dresselhaus G and Avouris P 2001 *Carbon Nanotubes: Synthesis, Structure, Properties, and Applications* 1st edn (Berlin: Springer) (<https://doi.org/10.1007/3-540-39947-X>)
- [2] Schnorr J M and Swager T M 2010 Emerging applications of carbon nanotubes *Chem. Mater.* **23** 646–57
- [3] Terrones M 2003 Science and technology of the twenty-first century: synthesis, properties and applications of carbon nanotubes *Annu. Rev. Mater. Res.* **33** 419–501
- [4] Ledoux M-J and Pham-Huu C 2005 Carbon nanostructures with macroscopic shaping for catalytic applications *Catal. Today* **102–103** 2–14
- [5] Stevens R M 2009 New carbon nanotube AFM probe technology *Mater. Today* **12** 42–5
- [6] Harris P J F 2004 Carbon nanotube composites *Int. Mater. Rev.* **49** 31–43
- [7] Qian H, Greenhalgh E S, Shaffer M S P and Bismarck A 2010 Carbon nanotube-based hierarchical composites: a review *J. Mater. Chem.* **20** 4751–62
- [8] Baker R T K 1989 Catalytic growth of carbon filaments *Carbon* **27** 315–23
- [9] Greenhalgh E S 2009 *Failure Analysis and Fractography of Polymer Composites* (Cambridge: Woodhead Publishing Ltd)
- [10] Duncan R K 2008 Characterizing the reinforcement mechanisms in multiwall nanotube/polycarbonate composites across different length and time *PhD Thesis* Rensselaer Polytechnic Institute, New York
- [11] Herceg T M, Zainol Abidin M S, Greenhalgh E S, Shaffer M S P and Bismarck A 2016 Thermosetting hierarchical composites with high carbon nanotube loadings: en route to high performance *Compos. Sci. Technol.* **127** 134–41
- [12] He X D, Zhang F H, Wang R G and Liu W B 2007 Preparation of a carbon nanotube/carbon fiber multi-scale reinforcement by grafting multi-walled carbon nanotubes onto the fibers *Carbon* **45** 2559–63

- [13] Laachachi A, Vivet A, Nouet G, Ben Doudou B, Poilane C, Chen J, Bai J B and Ayachi M 2008 A chemical method to graft carbon nanotubes onto a carbon fiber *Mater. Lett.* **62** 394–7
- [14] Zhang F-H, Wang R-G, He X-D, Wang C and Ren L-N 2009 Interfacial shearing strength and reinforcing mechanisms of an epoxy composite reinforced using a carbon nanotube/carbon fiber hybrid *J. Mater. Sci.* **44** 3574–7
- [15] Rodriguez A J, Guzman M E, Lim C-S and Minaie B 2011 Mechanical properties of carbon nanofiber/fiber-reinforced hierarchical polymer composites manufactured with multiscale-reinforcement fabrics *Carbon* **49** 937–48
- [16] Guo J, Lu C, An F and He S 2012 Preparation and characterization of carbon nanotubes/carbon fiber hybrid material by ultrasonically assisted electrophoretic deposition *Mater. Lett.* **66** 382–4
- [17] Siddiqui N, Sham M, Tang B, Munir A and Kim J 2009 Tensile strength of glass fibres with carbon nanotube-epoxy nanocomposite coating *Composites A* **40** 1606–14
- [18] Baker R T K, Barber M A, Harris P S, Feates F S and Waite R J 1972 Nucleation and growth of carbon deposits from the nickel catalyzed decomposition of acetylene *J. Catal.* **26** 51–62
- [19] Steiner S A, Li R and Wardle B L 2013 Circumventing the mechanochemical origins of strength loss in the synthesis of hierarchical carbon fibers *ACS Appl. Mater. Interfaces* **5** 4892–903
- [20] Kim K J, Yu W-R, Youk J H and Lee J 2012 Degradation and healing mechanisms of carbon fibers during the catalytic growth of carbon nanotubes on their surfaces *ACS Appl. Mater. Interfaces* **4** 2250–8
- [21] De Greef N, Magrez A, Couteau E, Locquet J-P, Forró L and Seo J W 2012 Growth of carbon nanotubes on carbon fibers without strength degradation *Phys. Status Solidi b* **249** 2420–3
- [22] Qian H, Kalinka G, Chan K L A, Kazarian S G, Greenhalgh E S, Bismarck A and Shaffer M S P 2011 Mapping local microstructure and mechanical performance around carbon nanotube grafted silica fibres: methodologies for hierarchical composites *Nanoscale* **3** 4759–67
- [23] Sager R J, Klein P J, Lagoudas D C, Zhang Q, Liu J, Dai L and Baur J W 2009 Effect of carbon nanotubes on the interfacial shear strength of T650 carbon fiber in an epoxy matrix *Compos. Sci. Technol.* **69** 898–904
- [24] Hung K H, Kuo W S, Ko T H, Tzeng S S and Yan C F C F 2009 Processing and tensile characterization of composites composed of carbon nanotube-grown carbon fibers *Composites A* **40** 1299–304
- [25] Qian H, Bismarck A, Greenhalgh S, Kalinka G and Shaffer M S P 2008 Hierarchical composites reinforced with carbon nanotube grafted fibers: the potential assessed at the single fiber level *Chem. Mater.* **20** 1862–9
- [26] Hung K H, Tzeng S S, Kuo W S, Wei B Q and Ko T H 2008 Growth of carbon nanofibers on carbon fabric with Ni nanocatalyst prepared using pulse electrodeposition *Nanotechnology* **19** 5602–9
- [27] De Riccardis M F, Carbone D, Makris T D, Giorgi R, Lisi N and Salernitano E 2006 Anchorage of carbon nanotubes grown on carbon fibres *Carbon* **44** 671–4
- [28] Makris T D, Giorgi R, Lisi N, Pilloni L, Salernitano E, De Riccardis M F and Carbone D 2005 Carbon nanotube growth on PAN- and pitch-based carbon fibres by HFCVD *Fullerenes Nanotubes Carbon Nanostruct.* **13** 383–92
- [29] Thostenson E T, Li W Z, Wang D Z, Ren Z F and Chou T W 2002 Carbon nanotube/carbon fiber hybrid multiscale composites *J. Appl. Phys.* **91** 6034–7
- [30] Yamamoto N, Guzman de Villoria R and Wardle B L 2012 Electrical and thermal property enhancement of fiber-reinforced polymer laminate composites through controlled implementation of multi-walled carbon nanotubes *Compos. Sci. Technol.* **72** 2009–15
- [31] Wicks S, de Villoria R and Wardle B 2010 Interlaminar and intralaminar reinforcement of composite laminates with aligned carbon nanotubes *Compos. Sci. Technol.* **70** 20–8
- [32] Qian H, Bismarck A, Greenhalgh E S and Shaffer M S P 2010 Carbon nanotube grafted silica fibres: characterising the interface at the single fibre level *Compos. Sci. Technol.* **70** 393–9
- [33] Qian H, Bismarck A, Greenhalgh E S and Shaffer M S P 2010 Synthesis and characterisation of carbon nanotubes grown on silica fibres by injection CVD *Carbon* **48** 277–86
- [34] Garcia E J, Wardle B L, Hart A J and Yamamoto N 2008 Fabrication and multifunctional properties of a hybrid laminate with aligned carbon nanotubes grown *in situ* *Compos. Sci. Technol.* **68** 2034–41
- [35] Veedu V P, Cao A Y, Li X S, Ma K G, Soldano C, Kar S, Ajayan P M and Ghasemi-Nejhad M N 2006 Multifunctional composites using reinforced laminae with carbon-nanotube forests *Nat. Mater.* **5** 457–62
- [36] Cao A Y, Veedu V P, Li X S, Yao Z L, Ghasemi-Nejhad M N and Ajayan P M 2005 Multifunctional brushes made from carbon nanotubes *Nat. Mater.* **4** 540–5
- [37] Chatzigeorgiou G, Efendiev Y and Lagoudas D 2011 Homogenization of aligned ‘fuzzy fiber’ composites *Int. J. Solids Struct.* **48** 2668–80
- [38] Wicks S S, Wang W, Williams M R and Wardle B L 2014 Multi-scale interlaminar fracture mechanisms in woven composite laminates reinforced with aligned carbon nanotubes *Compos. Sci. Technol.* **100** 128–35
- [39] Li R, Lachman N, Florin P, Wagner H D and Wardle B L 2015 Hierarchical carbon nanotube carbon fiber unidirectional composites with preserved tensile and interfacial properties *Compos. Sci. Technol.* **117** 139–45
- [40] An F, Lu C, Li Y, Guo J, Lu X, Lu H, He S and Yang Y 2012 Preparation and characterization of carbon nanotube-hybridized carbon fiber to reinforce epoxy composite *Mater. Des.* **33** 197–202
- [41] Song Q, Li K-Z, Li H-L, Li H-J and Ren C 2012 Grafting straight carbon nanotubes radially onto carbon fibers and their effect on the mechanical properties of carbon/carbon composites *Carbon* **50** 3949–52
- [42] Baker R T K, Chludzinski J J Jr and Sherwood R D 1985 A comparison of the catalytic influence of nickel, iron and nickel-iron on the gasification of graphite in various gaseous environments *Carbon* **23** 245–54
- [43] Hata K, Futaba D N, Mizuno K, Namai T, Yumura M and Iijima S 2004 Water-assisted highly efficient synthesis of impurity-free single-walled carbon nanotubes *Science* **306** 1362–4
- [44] Tomita A and Tamai Y 1972 Hydrogenation of carbons catalyzed by transition metals *J. Catal.* **27** 293–300
- [45] Magrez A, Seo J, Kuznetsov V and Forro L 2007 Evidence of an equimolar C₂H₂-CO₂ reaction in the synthesis of carbon nanotubes *Angew. Chem., Int. Ed. Engl.* **46** 441–4
- [46] De Greef N, Magrez A, Locquet J P, Forró L and Seo J K 2012 Grafting carbon nanotubes on carbon fibers without loss in carbon fibres strength, using the equimolar C₂H₂-CO₂ reaction *ECCM15—15th European Conf. on Composite Materials (Venice, Italy)* pp 1–6
- [47] Kudo A, Steiner S A, Bayer B C, Kidambi P R, Hofmann S, Strano M S and Wardle B L 2014 CVD growth of carbon nanostructures from zirconia: mechanisms and a method for enhancing yield *J. Am. Chem. Soc.* **136** 17808–17
- [48] Tyagi P K, Janowska I, Cretu O, Pham-Huu C and Banhart F 2011 Catalytic action of gold and copper crystals in the growth of carbon nanotubes *J. Nanosci. Nanotechnol.* **11** 3609–15

- [49] Inoue Y, Naito K, Koyama M, Fukuda H and Kagawa Y 2012 The effect of carbon nanotube grafted on the tensile, shear and peel properties of polyacrylonitrile-based carbon fibre/epoxy bundle composites *ECCM15—15th European Conf. on Composite Materials (Venice, Italy)* pp 1–6
- [50] Naito K, Yang J-M, Tanaka Y and Kagawa Y 2008 Tensile properties of carbon nanotubes grown on ultrahigh strength polyacrylonitrile-based and ultrahigh modulus pitch-based carbon fibers *Appl. Phys. Lett.* **92** 1912–3
- [51] Naito K, Yang J-M, Xu Y and Kagawa Y 2010 Enhancing the thermal conductivity of polyacrylonitrile- and pitch-based carbon fibers by grafting carbon nanotubes on them *Carbon* **48** 1849–57
- [52] Hu J, Dong S, Wu B, Zhang X, Wang Z, Zhou H, He P, Yang J and Li Q 2013 Mechanical and thermal properties of Cf/SiC composites reinforced with carbon nanotube grown *in situ* *Ceram. Int.* **39** 3387–91
- [53] Li K-Z, Song Q, Qiang Q and Ren C 2012 Improving the oxidation resistance of carbon/carbon composites at low temperature by controlling the grafting morphology of carbon nanotubes on carbon fibres *Corros. Sci.* **60** 314–7
- [54] An F, Lu C, Guo J, He S, Lu H and Yang Y 2011 Preparation of vertically aligned carbon nanotube arrays grown onto carbon fiber fabric and evaluating its wettability on effect of composite *Appl. Surf. Sci.* **258** 1069–76
- [55] Vogel S, Dransfeld C, Fiedler B and Gobrecht J 2014 Protective effect of thin alumina layer on carbon fibre to preserve tensile strength during CNT growth by CVD *ECCM16—16th European Conf. Comp. Mater. (Seville, Spain)* pp 1–7
- [56] Boroujeni A Y, Tehrani M, Nelson A J and Al-Haik M 2014 Hybrid carbon nanotube–carbon fiber composites with improved in-plane mechanical properties *Composites B* **66** 475–83
- [57] de Resende V G, Antunes E F, de Oliveira Lobo A, Oliveira D A L, Trava-Airoldi V J and Corat E J 2010 Growth of carbon nanotube forests on carbon fibers with an amorphous silicon interface *Carbon* **48** 3655–8
- [58] Delmas M, Pinault M, Patel S, Porterat D, Reynaud C and Mayne-L’Hermite M 2012 Growth of long and aligned multi-walled carbon nanotubes on carbon and metal substrates *Nanotechnology* **23** 105604
- [59] Moon C-W, Meng L-Y, Im S-S, Rhee K-Y and Park S-J 2011 Improvement of the electrical conductivity of carbon fibers through the growth of carbon nanofibers *J. Nanosci. Nanotechnol.* **11** 6193–7
- [60] Patton S T, Zhang Q, Qu L, Dai L, Voevodin A A and Baur J 2009 Electromechanical characterization of carbon nanotubes grown on carbon fiber *J. Appl. Phys.* **106** 104313–9
- [61] Qu L T, Zhao Y and Dai L M 2006 Carbon microfibers sheathed with aligned carbon nanotubes: towards multidimensional, multicomponent, and multifunctional nanomaterials *Small* **2** 1052–9
- [62] Storck S, Malecki H, Shah T and Zupan M 2011 Improvements in interlaminar strength: a carbon nanotube approach *Composites B* **42** 1508–16
- [63] Tehrani M, Boroujeni A Y, Luhrs C, Phillips J and Al-Haik M S 2014 Hybrid composites based on carbon fiber/carbon nanofilament reinforcement *Materials* **7** 4182–95
- [64] Cartwright R J, Esconjauregui S, Weatherup R S, Hardeman D, Guo Y, Wright E, Oakes D, Hofmann S and Robertson J 2014 The role of the $sp^2:sp^3$ substrate content in carbon supported nanotube growth *Carbon* **75** 327–34
- [65] Rinaldi A, Tessonier J-P, Schuster M E, Blume R, Girgsdies F, Zhang Q, Jacob T, Hamid S B A, Su D S and Schlögl R 2011 Dissolved carbon controls the initial stages of nanocarbon growth *Angew. Chem., Int. Ed.* **50** 3313–7
- [66] Joselevich E, Dai H J, Liu J, Hata K and Windle A H 2008 *Carbon Nanotube Synthesis and Organization* (Berlin: Springer) (https://doi.org/10.1007/978-3-540-72865-8_4)
- [67] Liu Z, Jiao L, Yao Y, Xian X and Zhang J 2010 Aligned, ultralong single-walled carbon nanotubes: from synthesis, sorting, to electronic devices *Adv. Mater.* **22** 2285–310
- [68] Huang L, Jia Z and O’Brien S 2007 Orientated assembly of single-walled carbon nanotubes and applications *J. Mater. Chem.* **17** 3863–74
- [69] Dai L, Patil A, Gong X, Guo Z, Liu L, Liu Y and Zhu D 2003 Aligned nanotubes *ChemPhysChem* **4** 1150–69
- [70] Merkulov V, Melechko A, Guillorn M, Lowndes D and Simpson M 2002 Effects of spatial separation on the growth of vertically aligned carbon nanofibers produced by plasma-enhanced chemical vapor deposition *Appl. Phys. Lett.* **80** 476–8
- [71] Chhowalla M, Teo K B K, Ducati C, Rupesinghe N L, Amaratunga G A J, Ferrari A C, Roy D, Robertson J and Milne W I 2001 Growth process conditions of vertically aligned carbon nanotubes using plasma enhanced chemical vapor deposition *J. Appl. Phys.* **90** 5308–17
- [72] Teo K B K *et al* 2004 The significance of plasma heating in carbon nanotube and nanofiber growth *Nano Lett.* **4** 921–6
- [73] Melechko A V, Merkulov V I, McKnight T E, Guillorn M A, Klein K L, Lowndes D H and Simpson M L 2005 Vertically aligned carbon nanofibers and related structures: controlled synthesis and directed assembly *J. Appl. Phys.* **97** 041301–39
- [74] Bao Q L and Pan C X 2006 Electric field induced growth of well aligned carbon nanotubes from ethanol flames *Nanotechnology* **17** 1016–21
- [75] Gao Y, Zhou Y S, Xiong W, Mahjouri-Samani M, Mitchell M and Lu Y F 2009 Controlled growth of carbon nanotubes on electrodes under different bias polarity *Appl. Phys. Lett.* **95** 143117
- [76] Hongo H, Nihey F and Ochiai Y 2007 Horizontally directional single-wall carbon nanotubes grown by chemical vapor deposition with a local electric field *J. Appl. Phys.* **101** 9
- [77] Neyts E C, van Duin A C T and Bogaerts A 2011 Insights in the plasma-assisted growth of carbon nanotubes through atomic scale simulations: effect of electric field *J. Am. Chem. Soc.* **134** 1256–60
- [78] Nojeh A, Ural A, Pease R F and Dai H J 2004 Electric-field-directed growth of carbon nanotubes in two-dimensions *J. Vac. Sci. Technol. B* **22** 3421–5
- [79] Ural A, Li Y and Dai H 2002 Electric-field-aligned growth of single-walled carbon nanotubes on surfaces *Appl. Phys. Lett.* **81** 3464–6
- [80] Wang H Z and Ren Z F 2011 The evolution of carbon nanotubes during their growth by plasma enhanced chemical vapor deposition *Nanotechnology* **22** 5601–6
- [81] Zhang Y G, Chang A L, Cao J, Wang Q, Kim W, Li Y M, Morris N, Yenilmez E, Kong J and Dai H J 2001 Electric-field-directed growth of aligned single-walled carbon nanotubes *Appl. Phys. Lett.* **79** 3155–7
- [82] Smiljanic O, Dellero T, Serventi A, Lebrun G, Stansfield B L, Dodelet J P, Trudeau M and Désilets S 2001 Growth of carbon nanotubes on ohmically heated carbon paper *Chem. Phys. Lett.* **342** 503–9
- [83] Kim H, Bae M, Kim Y, Cho E, Sohn Y and Kim D 2011 Growth of carbon nanotube field emitters on single strand carbon fiber: a linear electron source *Nanotechnology* **22** 95602
- [84] Pollack H W 1988 *Materials Science and Metallurgy* 4th edn (Englewood Cliffs, NJ: Prentice-Hall)
- [85] Abbaschian R, Abbaschian L and Reed-Hill R E 2009 *Physical Metallurgy Principles* 4th edn (Stamford: Cengage Learning)

- [86] Davies R H, Dinsdale A T, Gisby J A, Robinson J A J and Martin S M 2002 MTDATA - thermodynamics and phase equilibrium software from the National Physical Laboratory *CALPHAD Comput. Coupling Phase Diagr. Thermochem.* **26** 229–71
- [87] Schneider C A, Rasband W S and Eliceiri K W 2012 NIH Image to ImageJ: 25 years of image analysis *Nat. Meth.* **9** 671–5
- [88] BS ISO 11566 1996 *Carbon Fibre—Determination of the Tensile Properties of Single-Filament Specimens* (British Standards Institution) 1–5
- [89] Stoner E G, Edie D D and Durham S D 1994 An end-effect model for the single-filament tensile test *J. Mater. Sci.* **29** 6561–74
- [90] Du X, Liu H-Y, Zhou C, Moody S and Mai Y-W 2012 On the flame synthesis of carbon nanotubes grafted onto carbon fibers and the bonding force between them *Carbon* **50** 2347–50
- [91] Kim K J, Kim J, Lee G S, Jeon S-Y and Yu W-R 2012 Microstructure and bonding strength of carbon nanotubes directly grown on a carbon fibre substrate *ECCM15—15th European Conf. On Composite Materials (Venice, Italy)* pp 1–6
- [92] ISO 9277 2010 *Determination of the Specific Surface Area of Solids by Gas Adsorption—BET Method* (British Standards Institution) 1–24
- [93] Dresselhaus M S, Dresselhaus G, Saito R and Jorio A 2005 Raman spectroscopy of carbon nanotubes *Phys. Rep.* **409** 47–99
- [94] Suarez-Martinez I, Grobert N and Ewels C P 2012 Nomenclature of sp² carbon nanoforms *Carbon* **50** 741–7
- [95] Bunsell A R and Renard J 2005 *Fundamentals of Fibre Reinforced Composite Materials* (Bristol: Institute of Physics Publishing) (<https://doi.org/10.1201/9781420056969>)
- [96] Koziol K, Vilatela J, Moisala A, Motta M, Cunniff P, Sennett M and Windle A 2007 High-performance carbon nanotube fiber *Science* **318** 1892–5
- [97] Li P, Zhao Q, Zhou X, Yuan W and Chen D 2009 Enhanced distribution and anchorage of carbon nanofibers grown on structured carbon microfibers *J. Phys. Chem. C* **113** 1301–7
- [98] Chen C-C, Chen C F C F, Hsu C-H and Li I H 2005 Growth and characteristics of carbon nanotubes on carbon cloth as electrodes *Diam. Relat. Mater.* **14** 770–3
- [99] Menzel R, Lee A, Bismarck A and Shaffer M S P 2009 Inverse gas chromatography of as-received and modified carbon nanotubes *Langmuir* **25** 8340–8
- [100] Sing K S W, Everett D H, Haul R A W, Moscou L, Pierotti R A, Rouquerol J and Siemieniowska T 1985 Reporting physisorption data for gas/solid systems with special reference to the determination of surface area and porosity *Pure Appl. Chem.* **57** 603–19
- [101] An F, Lu C, Guo J and Lu H 2012 Preparation of CNT-hybridized carbon fiber by aerosol-assisted chemical vapor deposition *J. Mater. Sci.* **47** 3327–33
- [102] Vayenas C G, Bebelis S and Neophytides S 1988 Non-Faradaic electrochemical modification of catalytic activity *J. Phys. Chem.* **92** 5083–5
- [103] Frieder M and Jean-Christophe B 2005 Electrowetting: from basics to applications *J. Phys.: Condens. Matter* **17** R705–74
- [104] Quilliet C and Berge B 2001 Electrowetting: a recent outbreak *Curr. Opin. Colloid Interface Sci.* **6** 34–9
- [105] Verheijen H J J and Prins M W J 1999 Reversible electrowetting and trapping of charge: model and experiments *Langmuir* **15** 6616–20
- [106] Grill A 1994 *Cold Plasma Materials Fabrication: From Fundamentals to Applications* (New York: Wiley)
- [107] Lieberman M A and Lichtenberg A J 2005 *Principles of Plasma Discharges and Materials Processing* 2nd edn (New York: Wiley)
- [108] Lucas J R 1995 *High Voltage Engineering* (Sri Lanka: University of Moratuwa)
- [109] Bower C, Zhu W, Jin S and Zhou O 2000 Plasma-induced alignment of carbon nanotubes *Appl. Phys. Lett.* **77** 830–2
- [110] Merkulov V, Melechko A, Guillorn M, Simpson M, Lowndes D and Wheaton J 2002 Controlled alignment of carbon nanofibers in a large-scale synthesis process *Appl. Phys. Lett.* **80** 4816–8